

1 **Photoacoustic measurement may significantly overestimate NH<sub>3</sub> emissions from cattle**  
2 **houses due to VOC interferences**

3

4

5 Dezhao Liu<sup>1,2\*</sup>, Li Rong<sup>2</sup>, Jesper Kamp<sup>2</sup>, Xianwang Kong<sup>1</sup>, Anders Peter Adamsen<sup>3</sup>, Albarune

6 Chowdhury<sup>2</sup>, Anders Feilberg<sup>2\*</sup>

7

8 1- Zhejiang University, College of Biosystems Engineering and Food Science, Yuhangtang

9 Road 866, 310058 Hangzhou, China

10 2- Aarhus University, Department of Engineering, Finlandsgade 22, 8200 Aarhus N, Denmark

11 3- APSA, c/o Agro Business Park, Niels Pedersens Allé 2, DK-8830 Tjele, Denmark

12

13 **Corresponding author: Dezhao Liu: [dezhaoliu@zju.edu.cn](mailto:dezhaoliu@zju.edu.cn);**

14 **Anders Feilberg: [af@eng.au.dk](mailto:af@eng.au.dk)**

15

16

17

18

19

20

21

22

23 **Abstract:** Infrared photoacoustic spectroscopy (PAS) is a widely used method for measurement  
24 of NH<sub>3</sub> and greenhouse gas emissions especially in agriculture, but non-targeted gases such as  
25 volatile organic compounds (VOCs) from cattle barns may interfere with target gases causing  
26 inaccurate results. This study made an estimation of NH<sub>3</sub> interference in PAS caused by selected  
27 non-targeted VOCs which were simultaneously measured by a PAS and a PTR-MS (proton  
28 transfer reaction mass spectrometry). Laboratory calibration were performed for NH<sub>3</sub>  
29 measurement and VOCs were selected based on a headspace test of the feeding material maize  
30 silage. Various levels of interference of tested VOCs were observed on NH<sub>3</sub> and greenhouse  
31 emissions measured by the PAS. Particularly, ethanol, methanol, 1-butanol, 1-propanol and  
32 acetic acid were found to have highest interference on NH<sub>3</sub>. A linear response was typically  
33 obtained, with non-linear relation was however observed for VOCs on N<sub>2</sub>O emissions. The  
34 corrected online NH<sub>3</sub> concentrations measured by the PAS from a field study were confirmed  
35 to be reasonably correlated to the NH<sub>3</sub> concentration measured simultaneously by the PTR-MS.  
36 It was concluded that the correction factors could be used for possible data corrections when  
37 the concentrations of VOCs could be obtained by using e.g. PTR-MS.

## 38 **1 Introduction**

39 Measurements of ammonia and greenhouse emissions are gaining increased research attention  
40 in recent years due to stronger interests on global change and air pollution. Especially, ammonia  
41 not only causes serious environmental problems such as soil acidification as well as pollution  
42 of underground water and surface water with nitrogen eutrophication (van Breemen et al., 1983;  
43 Pearson and Stewart, 1993; Erisman et al., 2007), but is also important for fine particle  
44 formation (Bouwman et al., 1997; Seinfeld and Pandis, 1997; Pinder et al., 2007). The

45 greenhouse gas emissions, on the other hand, are causing climate change (Thomas et al., 2004;  
46 Chadwick et al., 2011). Livestock husbandry was estimated to be responsible for more than 80 %  
47 of the ammonia emission in Western Europe (Hutchings et al., 2001; EMEP, 2013) and more  
48 than 60% in China (Paulot et al., 2014). In the U.S., agriculture accounts for ~90 % of the total  
49 ammonia emissions (Aneja et al., 2009). Meanwhile, agriculture accounts for 52 and 84 % of  
50 global anthropogenic methane and nitrous oxide emissions (Smith et al., 2008). Accurate  
51 measurements of ammonia and greenhouse emissions are therefore vital for reliable emission  
52 estimation and thereby the possible reduction of these emissions through various efforts, such  
53 as air cleaning with biotrickling filters and air scrubbers (Melse and Van der werf, 2005; De  
54 Vries and Melse, 2017). For ammonia measurements, more than 30 % difference was observed  
55 when various methods were compared (Scholtens et al., 2004).

56 Infrared photoacoustic spectroscopy (PAS) is a widely-used technique for studies of air  
57 emissions especially within agriculture (Osada et al., 1998; Osada and Fukumoto, 2001;  
58 Emmenegger et al., 2004; Schilt et al., 2004; Heber et al., 2006; Elia et al., 2006; Blanes-Vidal  
59 et al., 2007; Hassouna et al., 2008; Rong et al., 2009; Ngwabie et al., 2011; Cortus et al., 2012;  
60 Joo et al., 2013; Wang-Li et al., 2013; Iqbal et al., 2013; Zhao et al., 2016; Ni et al., 2017; Lin  
61 et al., 2017). The PAS technique determines the gas concentrations through measuring acoustic  
62 signals caused by cell pressure change when gas inside absorbs energy from infrared light at a  
63 specific wavelength using the optical filter and expands (Iqbal et al., 2013). For example, the  
64 Innova 1312 (AirTech Instruments, Ballerup, Denmark) uses the PAS method and was  
65 previously verified by the US EPA and recommended by the Air Resources Board in California  
66 (CARB, 2000). Besides, PAS has the advantages of performing continuous measurement with

67 low maintenance and good selectivity and can simultaneously measure five compounds,  
68 typically including  $\text{NH}_3$ ,  $\text{CH}_4$ ,  $\text{CO}_2$  and  $\text{N}_2\text{O}$  for agricultural applications. The water vapor was  
69 usually also included in order to make proper concentration corrections when necessary.  
70 Nevertheless, since the infrared spectroscopic method is applied for measuring gas  
71 concentrations in PAS, the overlapping of IR spectra with non-targeted gases can introduce  
72 significant interferences due to the adsorption of infrared light at similar wavelengths, even  
73 though the infrared bands selected by optical filters are relatively narrow. The interferences can  
74 be corrected through cross-compensation for all target gases when the instrument is calibrated  
75 (Lumasense, 2012), but understanding and estimation of interferences from possible non-  
76 targeted gases is very important. This is especially important for field applications where the  
77 manure or the animal feed may emit various types of gases depending on the management and  
78 operations in the animal houses (Hafner et al., 2010; Moset et al., 2012). Until now, the PAS  
79 interference of has not been well estimated and corrected for, although interferences were  
80 previously suspected in livestock facilities (Phillips et al., 2001; Mathot et al., 2007; Ni & Heber,  
81 2008). Flechard et al. (2005) suspected that the  $\text{N}_2\text{O}$  concentration from soil measured by PAS  
82 (Innova 1312) was heavily influenced by  $\text{CO}_2$  and temperature even when cross-interference  
83 compensation was applied; they developed an alternative correction algorithm based on  
84 controlled  $\text{N}_2\text{O}/\text{CO}_2/\text{H}_2\text{O}$  ratios under selected temperature. Zhao et al (2012) claimed that the  
85 internal cross compensation could eliminate the interferences between target gases, and  
86 quantified interferences of non-targeted gas of  $\text{NH}_3$  on targeted gases of ethanol, methanol,  $\text{N}_2\text{O}$ ,  
87  $\text{CO}_2$ , and  $\text{CH}_4$ , however, without giving specific correction factors. Iqbal et al. (2013) also  
88 demonstrated that a careful calibration could eliminate the internal cross interferences of high

89 water vapor and CO<sub>2</sub> concentrations on low concentrations of N<sub>2</sub>O at the soil surface by  
90 comparison to GC measurements. Nevertheless, tests on interferences by non-targeted VOCs  
91 were not included in their study, likely due to the typical low concentrations of VOC in soil  
92 (Insam and Seewald, 2010). Hassouna et al. (2013) presented a field study on dairy cow  
93 buildings, where interferences on NH<sub>3</sub>, CH<sub>4</sub> and N<sub>2</sub>O were observed. The interferences were  
94 suspected to be caused by volatile organic compounds (VOCs; acetic acid, ethanol and 1-  
95 propanol) that they measured simultaneously; in their study, two PAS instruments were applied  
96 with one of them allocated with optical filters of these VOCs (NH<sub>3</sub> optical filter was included  
97 for both PAS). Still, no correction factors were given in terms of tested volatile organic  
98 compounds, which were typically emitted from feeding materials such as maize silage (Howard  
99 et al., 2010; Malkina et al., 2011). Opposite to what was claimed by some previous studies (e.g.,  
100 Heyden et al., 2016), the correction of interferences of non-targeted VOCs on NH<sub>3</sub> emission is  
101 also essential for the evaluation of emission abatement technologies such as air scrubbers,  
102 especially when the inlet VOC concentrations are relatively high. An overestimation of  
103 ammonia removal efficiency could easily be obtained since less interference would be expected  
104 for the outlet VOCs especially for water-soluble compounds such as the VOCs investigated in  
105 this study.

106 This study, therefore, performed an evaluation on ammonia measurements and interferences by  
107 non-targeted gases of volatile organic compound on targeted NH<sub>3</sub> and greenhouse gases  
108 measurement by PAS, with the interference on NH<sub>3</sub> simultaneously demonstrated by Proton-  
109 transfer-reaction mass spectrometry (PTR-MS), Cavity Ring-Down Spectroscopy (CRDS) and  
110 PAS. The experiments were as follows: (1) ammonia laboratory calibration by the three

111 instruments of PAS, PTR-MS and CRDS; (2) VOC selection test for non-targeted interference  
112 to ammonia by the PAS; (3) Effect of non-targeted VOCs on ammonia and greenhouse  
113 emissions measured by the PAS; (4) Field confirmation of interferences of non-targeted VOCs  
114 on ammonia measurement and data correction.

## 115 **2 Materials and methods**

### 116 **2.1 Instrumentation for gas concentrations measurement**

117 In this study, a PTR-MS, a CRDS NH<sub>3</sub> analyzer and a PAS gas analyzer were used to measure  
118 gas concentrations. PTR-MS is a state-of-the-art and widely used CIMS (short for chemical-  
119 ionization mass spectrometry) technique for highly sensitive online measurements of VOCs  
120 (De Gouw and Warneke, 2007; Blake et al., 2009; Yuan et al., 2017). PTR-MS can also measure  
121 a few inorganic compounds such as ammonia (at  $m/z$  18) since the proton affinity (204.0  
122 kcal/mol) of ammonia is higher than that of water (165.0 kcal/mol). Due to the fact that intrinsic  
123 ion at  $m/z$  18 could be formed in the plasma ion source (Norman et al., 2007), ammonia  
124 measurement by PTR-MS need to be evaluated carefully. For agricultural applications with  
125 relative high ammonia concentrations (e.g., Rong et al., 2009), this high background is usually  
126 not a big problem, since the typical background concentration is only a few hundred ppbv.  
127 When total gas concentration measured by PTR-MS is higher than approximately 10 ppmv,  
128 dilution is needed to keep the stable level of primary ion signals. A high-sensitivity PTR-MS  
129 (Ionicon Analytik GmbH, Innsbruck, Austria) was applied for the test of ammonia calibration  
130 in the laboratory, effects of non-targeted VOCs on ammonia measurement and field  
131 confirmation of interferences of non-targeted VOCs on ammonia measurement. Standard  
132 conditions with a total voltage of 600 V in the drift tube were utilized for the PTR-MS. Pressure

133 and temperature in the drift tube were maintained in the range of 2.1-2.2 mbar and at 60 °C,  
134 respectively, which gives an E/N ratio of ca. 135 Townsend. The inlet of the PTR-MS is PEEK  
135 tubing of 1.2 m length with 0.64 mm inner diameter (ID) and 1.6 mm outer diameter (OD). The  
136 inlet flow to the PTR-MS during calibration test and measurements was kept ~150 mL/min.  
137 The inlet temperature was maintained at 60 °C. Mass calibration was performed before each  
138 test, while transmission calibration was performed for every two weeks as suggested by the  
139 manufacturer.

140 CRDS determines the gas concentration (e.g., NH<sub>3</sub>) by measuring the acceleration of ring down  
141 time of light in the cavity due to absorption by a targeted gas species, this is compared to the  
142 ‘normal’ ring down time of the light introduced by a laser with tunable wavelength (von  
143 Bobruzki et al., 2010; Picarro, 2017). The very long effective path length of the light in the  
144 cavity (e.g., over 20 km for 25 cm cavity) (Picarro, 2017), enables a significantly higher  
145 sensitivity compared to conventional absorption spectroscopy (Berden et al., 2000; von  
146 Bobruzki et al., 2010). A G2103 Analyzer (Picarro Inc., Sunnyvale, CA, USA) using CRDS  
147 technique was applied in this study for the test of ammonia laboratory calibration and for the  
148 effect of non-targeted VOCs on ammonia measurement. The manufacturer calibrated the CRDS  
149 analyzer approximately 3 months before calibration tests and interference measurements. The  
150 CRDS analyzer was equipped with two in-line, sub-micron polytetrafluoroethylene (PTFE)  
151 particulate matter filters; one at the gas inlet at the back of the analyzer and one at the inlet of  
152 the cavity to protect the highly reflective mirrors. The inlet of the CRDS is a Teflon (PTFE)  
153 tubing of 1.5 m length with 6.4 mm outer diameter. Since molecular spectroscopy is  
154 fundamentally affected by temperature and pressure, the CRDS’s optical cavities incorporate

155 precise temperature and pressure control systems, with the measurement cell temperature  
156 controlled under precision of  $\pm 0.005$  °C, while the measurement cell pressure controlled  
157 under precision of  $\pm 0.0002$  atm. In this study, both the temperature and pressure of the air  
158 sample continuously flowing through the optical cavity are tightly controlled at all times to  
159 constant values of 45 °C and 140 Torr, respectively. The measurement interval is around 3  
160 seconds. The CRDS analyzer measured the water vapor simultaneously.

161 A photoacoustic multi-gas monitor 1312 (Innova, Lumasense Technology A/S, Denmark) using  
162 PAS technique was compared with the PTR-MS and the CRDS for ammonia calibration and  
163 non-targeted VOCs on ammonia measurement. The sample integration time to measure  
164 ammonia by the PAS was 20 s. The PAS used 6 optical filters including NH<sub>3</sub>, CH<sub>4</sub>, CO<sub>2</sub>, H<sub>2</sub>O,  
165 N<sub>2</sub>O and SF<sub>6</sub>. The specifications of the optical filters are shown in Table S1. Water vapor must  
166 be included for PAS measurement, since the absorbance spectrum of water overlap with other  
167 gases such as N<sub>2</sub>O and CO<sub>2</sub> thus causing interferences. The supplier calibrated the PAS before  
168 the conduction of the measurements for comparison in this study. The interferences between  
169 the target gases were therefore supposed to be eliminated through internal cross compensation  
170 (Lumasense, 2012; Zhao et al., 2012).

## 171 **2.2 Experiment 1: laboratory test on ammonia calibration**

172 The background measurement, calibration on selected ammonia concentrations, and reaction  
173 time and decay time measurement were performed for ammonia measurement by PAS, PTR-  
174 MS and CRDS. For the background measurement, zero air controlled by a mass flow controller  
175 (Bronkhorst, Ruurlo, The Netherlands) was supplied, and measurement was performed  
176 individually for each instrument. The selected ions measurement mode was used for the PTR-



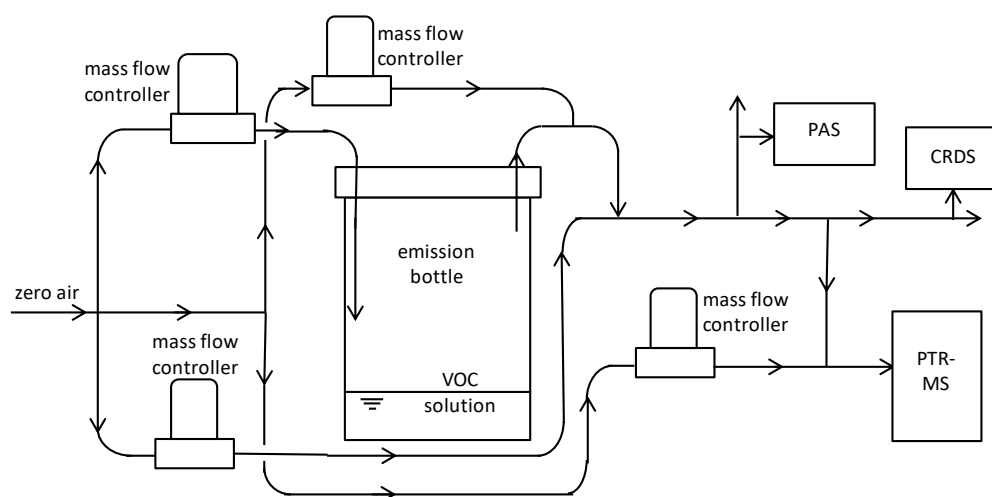
177 MS with m/z 18 being used for ammonia measurement. For the calibration test, a factory-  
178 calibrated gas cylinder (AGA A/S, Copenhagen, Denmark) containing 99.7 ( $\pm$  10 %) ppmv  
179 ammonia was used for the calibration test. Mass flow controllers (Bronkhorst, Ruurlo, The  
180 Netherlands) were used to dilute the cylinder gas with zero air to achieve the desired NH<sub>3</sub>  
181 concentration levels. For the decay time test, zero air flow was supplied to the instruments at  
182 first, then switched to a diluted flow (via 2-levels of mass flow controllers) with ammonia  
183 concentration around 5.2 ppmv supplying to all three instruments simultaneously, afterwards  
184 the ammonia supply flow was then set to zero to test the decay time. Four individual decay time  
185 tests were performed for the PAS, in order to confirm the long decay time of the instrument  
186 with low ammonia concentrations (5.2-8.8 ppmv) or high ammonia concentration (99.7 ppmv).  
187 For the reaction time test for the PAS, two different levels of ammonia concentration were  
188 introduced individually to the instrument, in order to test the dependence of the reaction time  
189 on ammonia concentration.

### 190 **2.3 Experiment 2: VOCs selection test**

191 In order to prepare the interferences test of non-targeted VOCs on ammonia measured by the  
192 PAS, a headspace test was performed and VOCs were selected through a PTR-MS measurement.  
193 Maize silage is a typical feeding material to the cows. A sample of maize silage was collected  
194 from the farm where the field confirmation experiment was performed (Skjern, Jutland,  
195 Denmark, altitude: 55°59'36.6", longitude: 8°29'53.52"). The silage was then transferred to the  
196 laboratory immediately for the headspace test. A clean plastic container (58×38×43 cm) with  
197 two oval holding holes on sides was used for the headspace test for VOCs selection. The  
198 container was half opened and the silage filled half of the container. A 1-meter 1/4-inch ID

199 PTFE tube was used for the test, with one end placed around 5 cm above the silage, and the  
 200 other side connected to a T-piece. One side of the T-piece was connected to a 1/8-inch ID PTFE  
 201 tube (around a half meter) which is connecting to the inlet of the PTR-MS. The flow rate of the  
 202 PTR-MS was kept at 150 mL/min. A zero-air dilution flow (75 mL/min) was supplied to the T-  
 203 piece in order to make 1:1 dilution to keep the total concentration below 10 ppmv. The  
 204 headspace measurement was performed by the PTR-MS on scan mode, and masses were  
 205 measured from 21 to 250 with 200 ms for each mass. The selection of VOCs was based on the  
 206 scan results and relevant literature for silage (Howard et al., 2010; Malkina et al., 2011).

207



208

209 **Figure 1.** The diagram of experimental set-up for ammonia interference calibration from VOCs.

210 **2.4 Experiment 3: Laboratory test for correction factors**

211 The diagram of the setup for the laboratory calibration test is shown in Figure 1. In the setup, a  
 212 pre-tested water solution containing the single VOC was purged from the headspace by zero air  
 213 (or nitrogen for one test on methanol), with flow controlled by a mass flow controller. The flow  
 214 was set with care, due to the relatively high sensitivity of VOC concentration on the purged gas  
 215 flow rate. One-liter airtight glass bottles were used for holding the water solution containing

216 the VOC, and 1/4-inch ID PTFE tube was used for the pipelines in the setup. The purged air  
217 flow in the PTFE tube containing a single VOC was diluted with air through a two-step dilution.  
218 The flows were adjusted according to the purged VOC concentration and the desired final VOC  
219 concentration. The pre-test for water solution preparation used a ratio of VOC:Water as 1:5,  
220 and the ratio between VOC and water was adjusted if the purged concentration after dilution  
221 (by zero air controlled by 2 mass flow controllers) measured by the PTR-MS was not within  
222 the desired range (too low or too high). For the laboratory calibration test, the diluted VOC was  
223 connected to the PAS, the CRDS and the PTR-MS for simultaneous measurements. In order to  
224 maintain stable pressures in the PAS and the CRDS, specific ranges of excess flow rates were  
225 required for these two instruments. Specific, the excess flow for the PAS was kept around 4 L  
226  $\text{min}^{-1}$ , while the excess flow for the CRDS was kept around 2 L  $\text{min}^{-1}$ . For the PTR-MS  
227 measurement, a further dilution by zero air was typically used to keep the total concentrations  
228 below 10 ppmv in order to avoid depletion of the primary ion,  $\text{H}_3\text{O}^+$ . Selected ion measurement  
229 mode was applied for the PTR-MS, with an integration time of 2 seconds for the tested VOC  
230 mass. During the experiments, the humidity was kept relatively low and stable, with dry zero  
231 air used for dilution for all cases, except for one test on methanol, which was also tested under  
232 nitrogen condition.

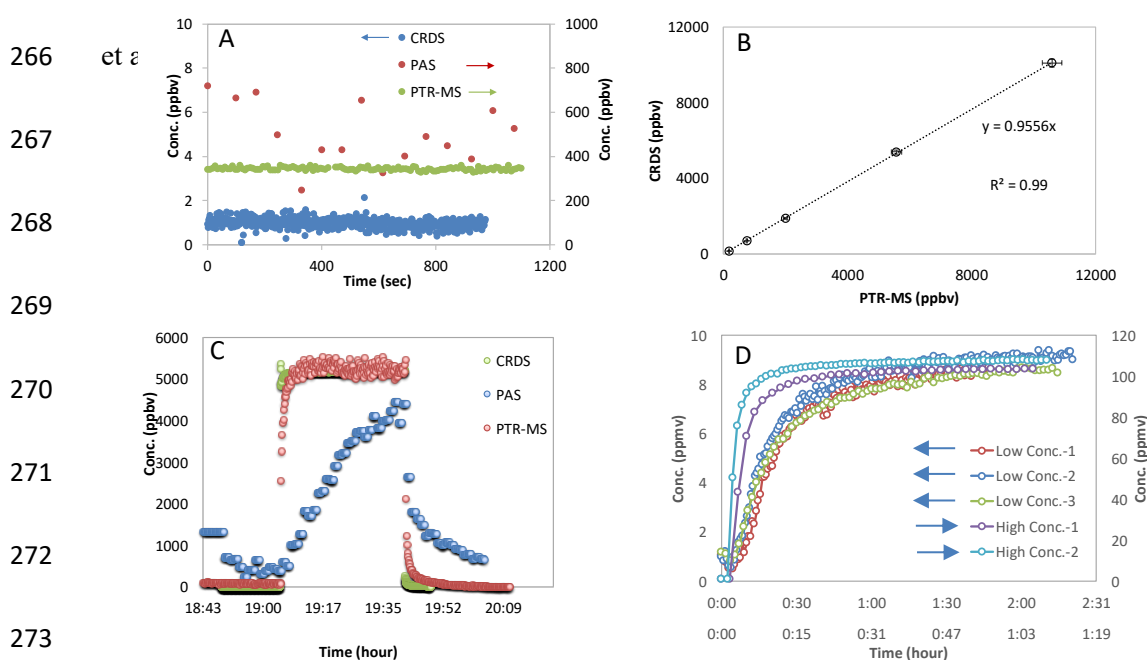
## 233 **2.5 Experiment 4: Field test for validation of correction factors**

234 The field demonstration test for non-targeted VOCs on ammonia measurement by the PAS was  
235 performed in the dairy farm mentioned above (Skjern, Jutland, Denmark), where both the PTR-  
236 MS and the PAS measured continuously. The dairy farm housed 360 cows with an average  
237 weight of 650 kg. The ventilation system consisted of natural and mechanical partial pit

238 ventilation system.

239 For the field test, the PAS was combined with a Multiplexer 1309 to measure from several  
240 sampling points. The PAS and the PTR-MS were placed in a movable trailer next to the dairy  
241 farm. The manufacturer calibrated the PAS instrument before the field test. The sample  
242 integration time was 5 s and the flushing time was 20 s. The air concentrations were measured  
243 by the PAS sequentially among two selected locations inside the farm, one location in the pit  
244 ventilation, one location outside the farm. Teflon tubes of 20 meters long and 8 mm OD were  
245 used for the sampling of air. The sampling lines were connected with the channels of the PAS  
246 multi-point sampler via continuously running Teflon membrane pumps to ensure constant  
247 flushing. Selected VOCs, odorants and NH<sub>3</sub> were measured simultaneously by the high  
248 sensitivity PTR-MS. Measurements were switched among the four measurement sampling lines  
249 and the background at ca. 10 min intervals via a custom-built switching box. PTFE tubes were  
250 used for the PTR-MS sampling lines, which were connected to Teflon sampling lines before the  
251 Teflon membranes pumps. The switching box was equipped with a five-port channel selector  
252 (Bio-Chem Valve Inc, USA) controlled automatically by 24V outputs from the PTR-MS. A  
253 PTFE tube (ID 1 mm) was used to connect the switching box to the inlet sampling line (1-meter  
254 PEEK tube with ID 0.64 mm) of the PTR-MS. For selected compounds, calibration was  
255 performed for the PTR-MS before the field measurements using permeation tubes and reference  
256 gas mixtures. Details regarding the calibration procedures could be found in our previous study  
257 (Feilberg et al., 2010). VOC concentrations were determined directly by the PTR-MS, based  
258 on estimated reaction rate constants described by Liu et al. (Liu et al., 2018). Standard  
259 conditions as described previously was applied and maintained for the PTR-MS. The mass

260 discrimination was calibrated and adjusted weekly by using a mixture of 14 aromatic  
 261 compounds between m/z (mass to charge ratio) 79 and 181 (P/N 34423-PI, Restek, Bellefonte,  
 262 PA). Selected ions were monitored with dwell time between 200 and 2000 ms during each  
 263 measurement cycle. Masses and dwell time selection was based on ion abundance in full scan  
 264 mode, relevant literature and experience regarding odorant compounds from dairy buildings as  
 265 well as from pig houses and pig slurry applications (Shaw et al., 2007; Chung et al., 2009; Liu



274

275 **Figure 2.** The calibration test of ammonia by the PAS, the PTR-MS and the CRDS. A: Background  
 276 comparison for the CRDS, the PAS and the PTR-MS for ammonia measurement; B: The calibration  
 277 of ammonia measured by the PTR-MS and by the CRDS; C: The instrument decay time of measured  
 278 ammonia concentration by the PTR-MS, the PAS and the CRDS; D: The reaction time for ammonia  
 279 for the PAS under low concentration (3 tests; ~8.9 ppmv) and high concentration (2 tests; 99.7 ppmv)  
 280 conditions (Low Conc.-1, Low Conc.-2 and Low Conc.-3 point to the vertical axis on the left,  
 281 and to the upper horizontal axis; High Conc.-1 and High Conc.-2 point to the vertical axis on the right,  
 282 and to the lower horizontal axis; High Conc.-2 was tested without the multiplexer).

283

### 284 3 Results and discussion

#### 285 3.1 Experiment 1: laboratory test on ammonia calibration

286 The background concentrations of ammonia measured by PAS, CRDS and PTR-MS,  
 287 respectively, are shown in Figure 2A, in which very low background concentration was  
 288 observed for the CRDS instrument (around 1 ppbv; 5 s) with detection limit around 0.67 ppbv  
 289 (3 times the standard deviation of the background). The PTR-MS, on the other hand, gave much  
 290 higher background with nearly 400 ppbv observed. The high background for ammonia  
 291 measured from the PTR-MS is caused by the intrinsic formation of  $\text{NH}_4^+$  ( $m/z$  18) in the ion  
 292 source (Norman et al., 2007). Nevertheless, the measured background signals for ammonia by  
 293 the PTR-MS was very stable and could be subtracted to give a detection limit of 21 ppbv (3  
 294 times the standard deviation of the background). Among the three instruments, the PAS gave  
 295 the highest background signal for ammonia (corresponding to  $502 \pm 140$  ppb), with a detection  
 296 limit around 421 ppbv (3 times the standard deviation of the background).

297 For the calibration test of ammonia, the ammonia concentrations measured by the CRDS and  
 298 the PTR-MS is shown in Figure 2B, in which the linearity ( $k = 0.9556$ ) and high correlation  
 299 ( $R^2=0.999$ ) are satisfactory for both instruments. The measured ammonia concentrations also  
 300 agreed with expected ammonia concentrations from the ammonia gas cylinder diluted in zero  
 301 air.

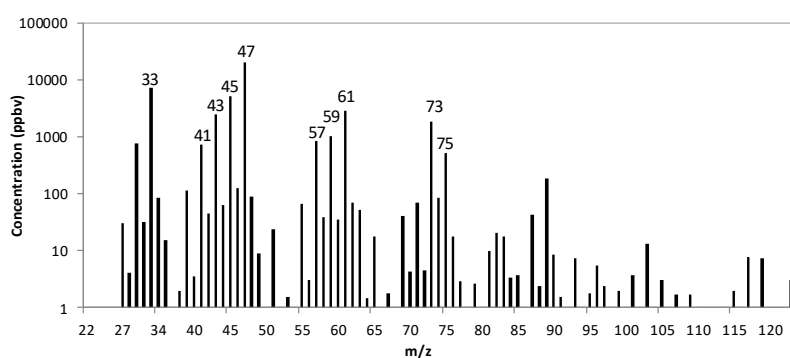
302 **Table 1.** Instrumental decay time (in second).

Unit (s)	PTR-MS (5.2 ppm)	Picarro (5.2 ppm)	Innova (5.2–8.8 ppm)	Innova (100 ppm)
90% decay	70–80	4.5–4.7	1700–4000	450–550

304

305 For the decay time test, the instrument decay times for ammonia measurements by the PAS, the  
 306 CRDS and the PTR-MS were measured simultaneously under a calibrated ammonia  
 307 concentration of 5.2 ppmv. As shown in Figure 2C, ammonia measured by the CRDS showed

308 the shortest decay time while the PAS gave the longest decay time. The estimated decay time  
 309 is shown in Table 1, in which the 90% decay time for ammonia measured by the CRDS is  
 310 around 4.5 - 4.7 second, with the 90% decay time from the PTR-MS estimated to be 70 to 80  
 311 seconds. The decay time for ammonia measured by the PAS showed remarkably longer, with  
 312 estimated 90% decay time around 1700 to 4000 seconds (for four individual tests with ammonia  
 313 concentration ranged from 5.2 to 8.8 ppmv). When much higher ammonia concentration was  
 314 used (99.7 ppmv), the 90% decay times measured by the PAS were apparently shorter (450 to  
 315 550 seconds). This result is consistent with the reaction time tests under two levels of input  
 316 ammonia concentrations (~ 8.9 ppmv and 99.7 ppmv, respectively), with the reaction time  
 317 comparably much shorter when input ammonia concentration is higher, as shown in Figure 2D.  
 318 Besides, the multiplexer attached to the PAS seemed to increase the reaction time, as also shown  
 319 in Figure 2D. However, a very high concentration of about 100 ppm is not expected to be  
 320 commonly seen in agricultural applications.



321  
 322 **Figure 3.** A scan example of the feeding material of silage by using headspace technique measured by  
 323 the PTR-MS. The m/z 47 is corrected for ethanol fragmentations formed in the PTR-MS through  
 324 calibration. Selected VOCs for the test in this study were ethanol, methanol, acetaldehyde, acetic acid,  
 325 2-butanone, acetone, propanol and butanol.

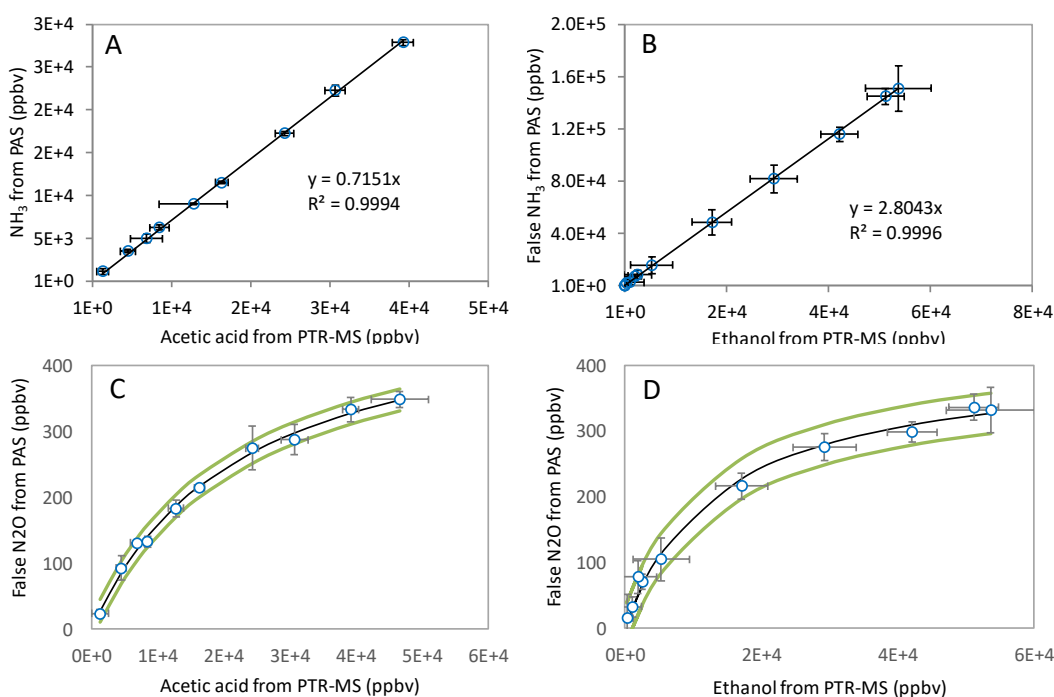
326

327 **3.2 Experiment 2: VOCs selection test**

328 The tested VOCs were selected according to a scan test of the headspace from the feeding

329 material of maize silage performed by the PTR-MS, as shown in Figure 3. The concentrations  
 330 shown in the figure were corrected for dilution, while the concentration of mass 47 was  
 331 corrected also from the calibration factor by assuming the mass 47 was assigned to ethanol.  
 332 Due to the fragmentation of ethanol in the PTR-MS measurement, only a fraction of ethanol  
 333 could be detected on mass 47 (Aprea et al., 2007). The highest peaks of the scan were at masses:  
 334 47, 33, 45, 61, 43, 73, 59, 75, 57 and 41. From the VOCs typically found in the highest  
 335 concentrations in barns and feeding material (Shaw et al., 2007; Chung et al., 2009; Howard  
 336 et al., 2010; Malkina et al., 2011; Hafner et al., 2013) and the scan results, a list of VOCs were  
 337 selected. The following VOCs were selected for the interferences tests of non-targeted VOC on  
 338 ammonia measurement by the PAS: ethanol, methanol, acetaldehyde, acetic acid, 2-butanone,  
 339 acetone, 1-propanol and 1-butanol. Compounds such as ethanol, methanol, acetic acid and 1-  
 340 propanol were typically found in cattle barns and feeding materials in high concentrations  
 341 (Shaw et al., 2007; Ngwabie et al., 2008; Howard et al., 2010; Hafner et al., 2013).

342  
 343  
 344  
 345  
 346  
 347  
 348  
 349  
 350  
 351  
 352  
 353  
 354  
 355  
 356  
 357  
 358  
 359





360 **Figure 4.** Examples for the interference calibration from non-targeted VOC on NH<sub>3</sub> (A & B) and  
 361 N<sub>2</sub>O (C & D) measured by the PAS. The VOC concentration on horizontal axis was measured by  
 362 the PTR-MS, while the NH<sub>3</sub> and N<sub>2</sub>O concentrations on vertical axis were from false signals  
 363 measured meanwhile by the PAS. A: The interference calibration for acetic acid on NH<sub>3</sub>; B: The  
 364 interference calibration for ethanol (corrected for fragments through calibration) on NH<sub>3</sub>; C: The  
 365 interference calibration for ethanol (corrected for fragments through calibration) on N<sub>2</sub>O; D: The  
 366 interference calibration for acetic acid on N<sub>2</sub>O. In C & D, the red line indicated the fit curve by  
 367 equation  $y=kx/(x+m)$ , and the green and purple curves indicated 95% confidence range.

### 368 3.3 Experiment 3: Laboratory test for correction factors

369 The interference of non-targeted VOC on ammonia measurement by the PAS was investigated  
 370 through selected single VOC as the sole input measured simultaneously by PAS, PTR-MS and  
 371 CRDS, as shown in the setup in Figure 1. An example of the interference test can be seen in  
 372 Figure S1, where the three instruments measured acetic acid simultaneously under various  
 373 concentration levels. Concentration dependent interference was clear for acetic acid on PAS  
 374 ammonia measurements.

375 **Table 2.** Obtained correction factors (in equations) between tested non-targeted VOC and the false  
 376 signal measured by PAS. ‘y’ points to the false concentration measured by PAS, and ‘x’ points to  
 377 the VOC concentration. The value in the brackets indicated the correlation coefficient of the linear  
 378 fit. N is the number of VOC concentration levels tested for determination of correction factors.

Compound	N	NH <sub>3</sub> (y: ppbv; x: ppbv)	CH <sub>4</sub> (y: ppbv; x: ppbv)	N <sub>2</sub> O (y: ppbv; x: ppmv)	CO <sub>2</sub> (y: ppbv; x: ppbv)	SF <sub>6</sub> (y: ppbv; x: ppbv)
ethanol	10	$y=2.81x(1.00)$	$y=1.88x(1.00)$	$y=411x/(x+14)(0.93)$	$y=0.40x(0.99)$	$y=-0.014x(1.00)$
methanol	9	$y=3.29x(0.74)$	$y=3.81x(0.74)$	$y=99x/(x+9)(0.78)$	$y=0.45x(0.47)$	$y=-0.15x(0.73)$
acetic acid	10	$y=0.72x(1.00)$	$y=-3.14x(1.00)$	$y=514x/(x+22)(0.95)$	$y=0.39x(0.99)$	$y=0.31x(1.00)$
acetaldehyde	4	(-)	$y=-0.85x(0.61)$	$y=317x/(x+31)(0.98)$	(-)	$y=0.044x(0.58)$
2-butanone	4	$y=-0.13x(1.00)$	$y=-4.02x(1.00)$	$y=311x/(x+26)(1.00)$	$y=-0.61x(0.74)$	$y=0.23x(1.00)$
acetone	6	$y=0.02x(0.99)$	$y=2.10x(0.99)$	$y=104x/(x+4)(0.99)$	(-)	$y=0.015x(0.99)$
1-propanol	5	$y=2.41x(0.87)$	$y=2.95x(0.87)$	$y=3569x/(x+602)(1.00)$	$y=0.25x(0.51)$	$y=-0.064x(0.84)$
1-butanol	7	$y=2.66x(0.99)$	$y=3.07x(0.99)$	$y=807x/(x+73)(0.99)$	(-)	$y=-0.061x(0.97)$
379 methanol(N <sub>2</sub> )	4	$y=1.03x(0.80)$	$y=1.46x(0.83)$	(-)	$y=0.35x(0.54)$	$y=-0.056x(0.86)$

380

381 In principle, establishing correction factors for each specific compound could eliminate the  
 382 interferences of VOCs on ammonia measurements on a specific instrument with the same filter  
 383 specifications. This requires, however, that VOC concentrations be measured simultaneously.

384 Figure 4A & B show two examples of the calibration lines for acetic acid and ethanol, from  
385 which a correction factor (CF) between the false ammonia concentration and the tested  
386 compound could be obtained (CF=0.72 for acetic acid and CF=2.81 for ethanol). A linear  
387 response of the ammonia interference was observed for all the tested compounds and they had  
388 high correlation coefficients. The correction factors for ammonia interference by other tested  
389 VOCs can be found in Table 2, where ethanol, methanol, 1-propanol and 1-butanol give the  
390 highest false signals on ammonia measured by the PAS, with correction factors of 2.81, 3.29,  
391 2.41 and 2.66, respectively. Due to the fact that these compounds are often found in cattle barn  
392 buildings and feed silage even in the level of ppmv especially for ethanol, methanol and 1-  
393 propanol (Rabaud et al., 2003; Ngwabie et al., 2008; Howard et al., 2010; Hafner et al., 2013),  
394 severe interference on ammonia measured by PAS could therefore exist. While acetic acid gave  
395 significant false signals on ammonia (CF=0.72), acetone only showed little interference on  
396 ammonia (CF=0.02). Meanwhile, negative false signals were observed for ammonia by 2-  
397 butanone (CF=-0.13). Interestingly, the correction factor for false ammonia by methanol in  
398 nitrogen matrix is significantly different from that by methanol presented in air matrix  
399 (CF=1.03 vs 3.29). This observation is possibly related to the relatively rapid vibrational energy  
400 transfer between the VOC and oxygen (Harren et al., 2000). While nitrogen has a vibrational  
401 frequency around  $2360\text{ cm}^{-1}$ , oxygen has a vibrational frequency of  $1554\text{ cm}^{-1}$  with only 170  
402 collisions needed to transfer energy to the vibrational mode of  $\text{O}_2$  (Lambert, 1977).

403 Besides the interferences on ammonia by the non-targeted VOCs, other target gases also  
404 showed various levels of interferences, as also indicated by previous studies (e.g., Zhao et al.,  
405 2012; Hassouna et al., 2013). Because target gases may have more overlap for the infrared

406 spectrum, the primary interference on one target gas caused by the overlap with non-targeted  
407 VOCs could therefore influence and cause secondary interference on other target gases (Zhao  
408 et al., 2012). Still, in theory, correction factors could be obtained for the interfered gases by the  
409 tested VOCs. Specifically, for the interference on methane by non-targeted methanol, 1-butanol,  
410 1-propanol, acetone and ethanol showed positive false signals (CF=3.81, 3.07, 2.95, 2.10, 1.88,  
411 respectively). 2-butanone, acetic acid and acetaldehyde showed negative false signals to  
412 methane, with correction factors equal to -4.02, -3.14 and -0.85, respectively. All interferences  
413 on methane are shown in Table 2. For methanol in nitrogen, the calibration again showed  
414 significant difference compared to air (CF=1.46 vs. 3.81).

415 Meanwhile, the non-targeted VOC also caused false signals on nitrous oxide signals, with a  
416 much lower level of interference. Further, the calibrations of the nitrous oxide interference by  
417 the non-targeted VOCs seemed not to be following linear relationships. For examples, Figure  
418 4C & D showed the false signals of nitrous oxide caused by ethanol and acetic acid. Clearly, a  
419 non-linear relation exists between the nitrous oxide interference and VOC concentration. The  
420 curves could be well fitted to the non-linear equation of  $y=kx/(x+m)$ , where k could represent  
421 the maximum interference on nitrous oxide by the single VOC, m could represent the half-  
422 saturation constant indicating the level higher than which of the VOC concentration could cause  
423 half of the maximum interference on nitrous oxide. As shown in Table 2, all tested VOCs  
424 showed positive non-linear interference to the nitrous oxide signals, and 1-butanol showed the  
425 highest maximum interference on nitrous oxide. Interestingly, no interference was observed for  
426 nitrous oxide when methanol was presented in nitrogen matrix, while a relatively lower level  
427 of interference observed on nitrous oxide by methanol when presented in air matrix compared

428 to other tested VOC.

429 Furthermore, some of the tested non-targeted VOCs also caused interference on carbon dioxide  
430 measured by the PAS. The background of carbon dioxide was considered as unchanged during  
431 the interference tests. While methanol, ethanol, acetic acid and 1-propanol caused positive false  
432 signals for carbon dioxide measured by the PAS (CF = 0.45, 0.40, 0.39, 0.25, respectively), 2-  
433 butanone caused negative false signals with CF = -0.61 (Table 2). Other tested VOCs, including  
434 acetone, acetaldehyde and 1-butanol, did not show interferences on carbon dioxide measured  
435 by the PAS. This is likely because no overlap of the gas infrared adsorption spectra exists  
436 between these VOCs and carbon dioxide. As expected, methanol in nitrogen also caused  
437 interference on carbon dioxide (CF = 0.35) slightly lower than methanol in air.

438 Besides, SF<sub>6</sub> measurements were interfered by the tested non-targeted VOC, with lower  
439 correction factor obtained compared to NH<sub>3</sub>, CH<sub>4</sub>, N<sub>2</sub>O and CO<sub>2</sub>. Acetic acid and 2-butanone  
440 caused the highest interferences on SF<sub>6</sub>, with correction factors of 0.31 and 0.23, respectively.  
441 Other tested VOCs caused significantly less interference on SF<sub>6</sub>, among which methanol gave  
442 the highest negative correction factor of -0.15. Again, the methanol in nitrogen gave a  
443 significantly lower level of interference on SF<sub>6</sub> compared to methanol in air (CF = -0.056 vs -  
444 0.15).

445 Overall, the tested non-target VOCs in this study caused significant interference on target gases,  
446 where ammonia and methane showed the most interference. Even though less interference was  
447 observed for nitrous oxide, this could still cause problems due to the typically low concentration  
448 level of this compound in e.g. livestock facilities or soil (Iqbal et al., 2013; Rong et al., 2014).  
449 Nevertheless, the correction factors obtained from this study offer a possibility for correcting

450 for the interferences caused by the tested non-targeted VOCs, if the specific VOC  
451 concentrations are available from simultaneous measurements. For historical data this is apart  
452 from a few exceptions never the case.

453

454

455

456

457

458

459

460

461

462

463

464

465

466

467

468

469

470

471

472

473

474

475

476

477

478

479

480

### 481 3.4 Experiment 4: Field test for validation of correction factors

482 During the field test in the partially ventilated dairy barn, the ammonia measurements by PAS

483 and PTR-MS were compared between each other for one location in the pit and two locations

484 (Location One and Location Two) in the barn. Figure S2 showed the ammonia measured by

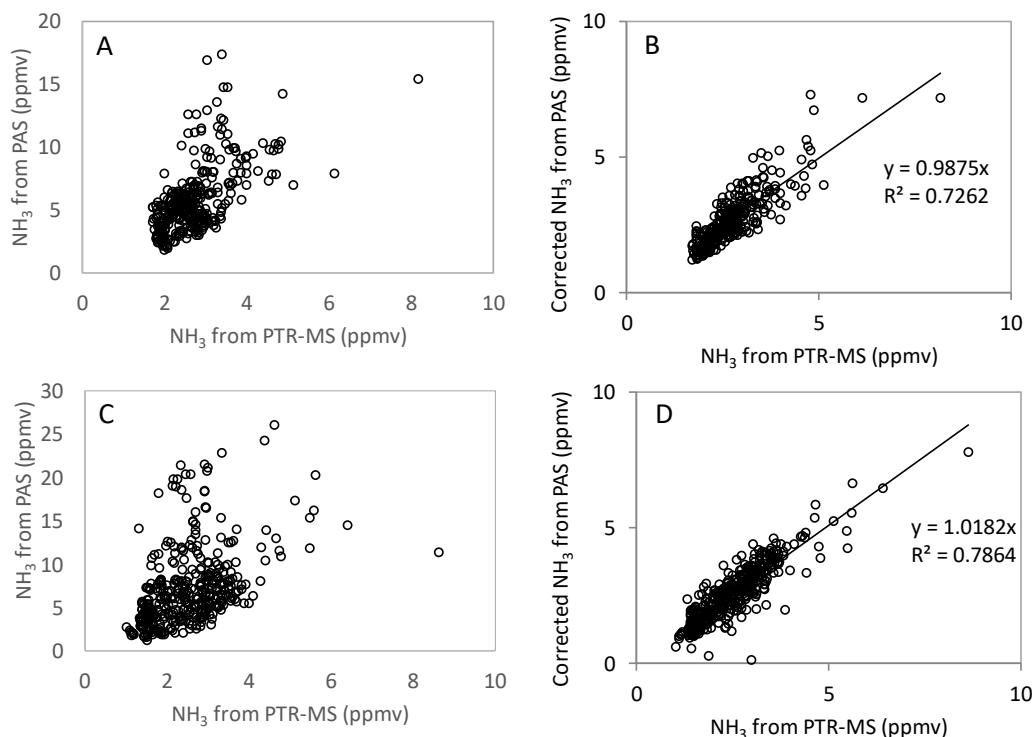


**Figure 5.** NH<sub>3</sub> concentrations measured by the PAS (vertical axis) and by the PTR-MS (horizontal axis) in the field measurement from Location One before the correction by the tested non-targeted VOCs (A) and after the correction by the tested non-targeted VOCs (B), and from Location Two before the correction by the tested non-targeted VOCs (C) and after the correction by the tested non-targeted VOCs (D).

485 PAS and PTR-MS at the measurement point of the pit ventilation. In the pit ventilation, low  
486 concentrations of VOCs were generally obtained and relatively high concentrations of ammonia  
487 were observed for both instruments. Thus, no significant interferences were observed for  
488 ammonia measured by the PAS, and ammonia measurements by PAS and PTR-MS showed a  
489 good agreement as shown in Figure S2. However, for the two measurement points inside the  
490 barn, significantly higher ammonia concentrations were obtained from PAS compared to the  
491 concentrations measured by PTR-MS (Figure 5 A & C). The higher ammonia concentration  
492 observed for the PAS measurement was most likely due to the interferences from VOCs, some  
493 of which had high concentrations, especially for ethanol as shown in Table 3. In fact, the relation  
494 between the ammonia concentrations measured by PAS and the ethanol concentrations  
495 measured by PTR-MS, were highly correlated for both measurement locations, with slopes  
496 close to 3 (2.97 and 3.12; see Figure S3). These two numbers are generally close to the  
497 correction factor obtained for ethanol ( $CF = 2.81$ ). The correction factors obtained in  
498 'Experiment 3' were used for data correction of ammonia measurement by PAS since the  
499 instrument configurations were kept the same. Thus, the interference of the VOCs on ammonia  
500 measurement by PAS could be estimated from the correction factors obtained in 'Experiment  
501 3' and used to correct the ammonia data. Figure 5B & D show the corrected ammonia  
502 concentrations measured by PAS by using the correction factors, together with the measured  
503 ammonia concentration by the PTR-MS for both measurement locations. The corrected  
504 ammonia concentrations from the PAS are generally in good agreement with the ammonia  
505 concentration measured by the PTR-MS, with slopes were close to 1 (0.99 and 1.02). This  
506 experiment validated that with the correction from major VOCs, the interference on  $NH_3$

507 measured by PAS could be reasonable estimated in field applications. However, it should be  
 508 noted that a lot of redundant work is needed to make this correction if only NH<sub>3</sub> concentration  
 509 determination needed, since a number of VOCs concentrations need to be known in order to  
 510 achieve a right correction even though some minor VOCs within low range ppbv could be  
 511 omitted.

512

513 **Table 3.** Average concentrations ( $\pm$  standard deviation) of selected VOCs during the field test in the  
 514 dairy cattle barn for the two sampling locations 1 & 2, both of which are located inside the barn.

Compound	Concentrations (ppbv)	
	Location 1	Location 2
ethanol	1421 $\pm$ 946	1622 $\pm$ 1355
methanol	237 $\pm$ 150	241 $\pm$ 192
acetic acid	57 $\pm$ 41	69 $\pm$ 62
acetaldehyde	99 $\pm$ 81	92 $\pm$ 84
2-butanone	19 $\pm$ 11	17 $\pm$ 13
acetone	78 $\pm$ 30	52 $\pm$ 25
1-propanol	71 $\pm$ 45	72 $\pm$ 68
1-butanol	22 $\pm$ 10	16 $\pm$ 12
hydrogen sulfide	12 $\pm$ 10	11 $\pm$ 8
trimethylamine	8.6 $\pm$ 3.5	5.7 $\pm$ 3.1
dimethyl sulfide	15 $\pm$ 9	14 $\pm$ 10
515 4-methylphenol	5.2 $\pm$ 2.1	3.8 $\pm$ 2.2

516

#### 517 **4 Conclusions**

518 One must take special care when measuring NH<sub>3</sub> and greenhouse gas emissions (CH<sub>4</sub>, N<sub>2</sub>O and  
 519 CO<sub>2</sub>) by using PAS techniques as Innova. Depending on the IR absorption spectra of different  
 520 gases, non-targeted gases such as VOCs may interfere significantly with the target gases  
 521 causing inaccurate results. In order to confirm and determine the correction factors regarding  
 522 the interference on targeted gases caused by selected VOCs, experiments were conducted by  
 523 using simultaneously a PAS and a PTR-MS, while also clarified by a CRDS. Results from these

524 experiments provide useful guidelines with regards to interferences caused by non-targeted  
525 gases. The results on correction factors revealed that the tested VOCs of ethanol, methanol, 1-  
526 butanol, 1-propanol and acetic acid caused the most significant interference on NH<sub>3</sub> measured  
527 by PAS. Interestingly, non-linear relations were obtained for interferences on N<sub>2</sub>O by test  
528 VOCs as non-targeted gases, while linear response was obtained for interference on other  
529 targeted gases. The field test in the cattle barn validated the interference caused by VOCs on  
530 NH<sub>3</sub> measurement by the PAS when simultaneously measured by the PTR-MS. Therefore, the  
531 correction factors could be used for potential data corrections when same type of PAS is used  
532 together with available VOCs data. No validation was performed for greenhouse emissions  
533 correction due to lack of alternative measurement.

534

535 *Code and data availability.* Data and code are available upon request to the corresponding  
536 author.

537 *Supplement.* The supplementary information is available free of charge at DOI: .

538

539 *Author contributions.* DL, LR and AF designed the setup for the experiments performed; LR,  
540 XK and AC contributed to setting up and conducting experiments and acquiring data; DL, AF,  
541 JK, XK and APA contributed to section writing and analysis; LR, AF and JK assisted in data  
542 analysis and manuscript editing.

543

544 *Competing interests.* The authors declare that they have no conflicts of interest.

545



546 *Acknowledgements.* This work was supported by National Natural Science Fund of China  
547 (No. 31672468) and Thousand Talents Program (Youth Project 2016).

548

#### 549 **References**

550 Aneja, V. P., Schlesinger, W. H., and Erisman, J. W.: Effects of agriculture upon the air quality  
551 and climate: research, policy, and regulations, *Environ. Sci. Technol.*, 43, 4234–4240,  
552 <https://doi.org/10.1021/es8024403>, 2009.

553 Angela, E., Di, F. C., Mario, L. P., and Gaetano, S.: Photoacoustic Spectroscopy with Quantum  
554 Cascade Lasers for Trace Gas Detection, *Sensors-Basel*, 6, 1411–1419,  
555 <https://doi.org/10.3390/s6101411>, 2006.

556 Aprea E., Biasioli F., Mark T.D., and Gasperi F.: PTR-MS study of esters in water and  
557 water/ethanol solutions: Fragmentation patterns and partition coefficients, *Int. J. Mass*  
558 *Spectrom.*, 262, 114–121, <https://doi.org/10.1016/j.ijms.2006.10.016>, 2007.

559 Berden, G., Peeters, R., and Meijer, G.: Cavity ring-down spectroscopy: Experimental schemes  
560 and applications, *Int. Rev. Phys. Chem.*, 19, 565–607,  
561 <https://doi.org/10.1080/014423500750040627>, 2000.

562 Blake, R. S., Monks, P. S., and Ellis, A. M.: Proton-transfer reaction mass spectrometry, *Chem.*  
563 *Rev.*, 109, 861–896, <https://doi.org/10.1002/chin.200923275>, 2009.

564 Blanes-Vidal, V., Topper, P. A., and Wheeler, E. F.: Validation of ammonia emissions from dairy  
565 cow manure estimated with a non-steady-state, recirculation flux chamber with whole-  
566 building emissions, *T. ASABE*, 50, 633–640, <https://doi.org/10.13031/2013.22652>, 2007.

567 Bouwman, A. F., Lee, D. S., Asman, W. A. H., Dentener, F. J., Van, D. H. K. W., and Olivier, J.

568 G. J.: A global high-resolution emission inventory for ammonia, *Global Biogeochem. Cy.*,  
569 11, 561–587, <https://doi.org/10.1029/97GB02266>, 1997.

570 California Air Resources Board (CARB).: Manufacturer Notification. Mail-Out #MSO 2000-  
571 08, CARB: Sacramento, CA, USA, Available online:  
572 <http://www.arb.ca.gov/msprog/mailouts/mso0008/mso0008.pdf>, 2000.

573 Chadwick, D., Sommer, S., Thorman, R., Fanguero, D., Cardenas, L., Amon, B., and  
574 Misselbrook, T.: Manure management: Implications for greenhouse gas emissions, *Anim.*  
575 *Feed Sci. Tech.*, 166-167, 514–531, <https://doi.org/10.1016/j.anifeedsci.2011.04.036>, 2011.

576 Chung, M.Y., Beene, M., Ashkan, S., Krauter, C., and Hasson, A.S.: Evaluation of non-enteric  
577 sources of non-methane volatile organic compound (NMVOC) emissions from dairies,  
578 *Atmos. Environ.*, 44, 786–794, <https://doi.org/10.1016/j.atmosenv.2009.11.033>, 2009.

579 Cortus E.L., Jacobson L.D., Hetchler B.P., and Heber A.J.: Emission monitoring methodology  
580 at a NAEMS dairy site, with an assessment of the uncertainty of measured ventilation rates,  
581 *ASABE - 9th International Livestock Environment Symposium*, 583-590,  
582 <https://doi.org/10.13031/2013.41578>, 2012.

583 De Gouw J., and Warneke C.: Measurements of volatile organic compounds in the earth's  
584 atmosphere using proton-transfer-reaction mass spectrometry, *Mass Spectrom. Rev.*, 26,  
585 223–257, <https://doi.org/10.1002/mas.20119>, 2007.

586 EMEP, Agency: EMEP/EEA air pollutant emission inventory guidebook - 2013. *Luxembourg:*  
587 *Publications Office of the European Union*, 3B: Manure management,  
588 [https://www.eea.europa.eu/publications/emep-eea-guidebook-2013/part-b-sectoral-](https://www.eea.europa.eu/publications/emep-eea-guidebook-2013/part-b-sectoral-guidance-chapters/4-agriculture/3-b-manure-management/view)  
589 [guidance-chapters/4-agriculture/3-b-manure-management/view](https://www.eea.europa.eu/publications/emep-eea-guidebook-2013/part-b-sectoral-guidance-chapters/4-agriculture/3-b-manure-management/view), 2013.

590 Emmenegger, L., Mohn J., Sigrist M., Marinov D., Steinemann U., Zumsteg F., and Meier M.:  
591 Measurement of ammonia emissions using various techniques in a comparative tunnel study,  
592 Int. J. Environ. Pollut., 22, 326–341, <https://doi.org/10.1504/IJEP.2004.005547>, 2004.

593 Erisman, J. W., Bleeker, A., Galloway, J., and Sutton, M. S.: Reduced nitrogen in ecology and  
594 the environment, Environ. Pollut., 150, 140–149,  
595 <https://doi.org/10.1016/j.envpol.2007.06.033>, 2007.

596 Feilberg A., Liu D., Adamsen A.P.S., Hansen M.J., and Jonassen K.E.N.: Odorant emissions  
597 from intensive pig production measured by online proton-transfer-reaction mass  
598 spectrometry, Environ. Sci. Technol., 44, 5894–5900, <https://doi.org/10.1021/es100483s>,  
599 2010.

600 Fle'chard, C. R., Neftel, A., Jocher, M., Ammann, C., and Fuhrer, J.: Bi-directional  
601 soil/atmosphere N<sub>2</sub>O exchange over two mown grassland systems with contrasting  
602 management practices, Global Change Biol., 11, 2114–2127, [https://doi.org/10.1111/j.1365-](https://doi.org/10.1111/j.1365-2486.2005.01056.x)  
603 [2486.2005.01056.x](https://doi.org/10.1111/j.1365-2486.2005.01056.x), 2010.

604 Hafner S.D., Howard C., Muck R.E., Franco R.B., Montes F., Green P.G., Mitloehner F., Trabue,  
605 S.L., and Rotz C.A.: Emission of volatile organic compounds from silage: Compounds,  
606 sources, and implications, Atmos. Environ., 77, 827–839,  
607 <https://doi.org/10.1016/j.atmosenv.2013.04.076>, 2013.

608 Hafner, S. D., Montes, F., Rotz, C. A., and Mitloehner, F.: Ethanol emission from loose corn  
609 silage and exposed silage particles. Atmos. Environ., 44, 4172–4180,  
610 <https://doi.org/10.1016/j.atmosenv.2010.07.029>, 2010.

611 Harren F.J.M., Cotti G., Oomens J., and Hekkert S.L.: Photoacoustic Spectroscopy in Trace Gas

612 Monitoring, in *Encyclopedia of Analytical Chemistry*, R.A. Meyers (Ed.), 2203–2226,  
613 ©JohnWiley & Sons Ltd, Chichester, 2000.

614 Hassouna, M., Espagnol, S., Robin, P., Paillat, J. M., Levasseur, P., and Li, Y.: Monitoring NH<sub>3</sub>,  
615 N<sub>2</sub>O, CO<sub>2</sub> and CH<sub>4</sub> emissions during pig solid manure storage and effect of turning,  
616 *Compost Sci. Util.*, 16, 267–274, <https://doi.org/10.1080/1065657X.2008.10702388>, 2008.

617 Hassouna, M., Robin, P., Charpiot, A., Edouard, N., and Méda, B.: Infrared photoacoustic  
618 spectroscopy in animal houses: Effect of non-compensated interferences on ammonia,  
619 nitrous oxide and methane air concentrations, *Biosyst. Eng.*, 114, 318–326,  
620 <https://doi.org/10.1016/j.biosystemseng.2012.12.011>, 2013.

621 Heber A.J., Ni J.-Q., Lim T.T., Tao P.-C., Schmidt A.M., Koziel J.A., Beasley D.B., Hoff, S.J.,  
622 Nicolai, R.E., Jacobson, L.D., and Zhang Y.: Quality assured measurements of animal  
623 building emissions: Gas concentrations, *J. Air Waste Manage.*, 56, 1472–1483,  
624 <https://doi.org/10.1080/10473289.2006.10465680>, 2006.

625 Heyden, C. V. D., Brusselman, E., Volcke, E. I. P., and Demeyer, P.: Continuous measurements  
626 of ammonia, nitrous oxide and methane from air scrubbers at pig housing facilities, *J.*  
627 *Environ. Manage.*, 181, 163–171, <https://doi.org/10.1016/j.jenvman.2016.06.006>, 2016.

628 Howard, C. J., Kumar, A., Malkina, I., Mitloehner, F., Green, P. G., Flocchini, R. G., and  
629 Kleeman, M. J.: Reactive organic gas emissions from livestock feed contribute significantly  
630 to ozone production in central California, *Environ. Sci. Technol.*, 44, 2309–2314,  
631 <https://doi.org/10.1021/es902864u>, 2010.

632 Hutchings, N. J., Sommer, S. G., Andersen, J. M., and Asman, W. A. H.: A detailed ammonia  
633 emission inventory for Denmark, *Atmos. Environ.*, 35, 1959–1968,

634 [https://doi.org/10.1016/S1352-2310\(00\)00542-2](https://doi.org/10.1016/S1352-2310(00)00542-2), 2001.

635 Insam, H., and Seewald, M. S. A.: Volatile organic compounds (VOCs) in soils, *Biol. Fert. Soils*,

636 46, 199–213, <https://doi.org/10.1007/s00374-010-0442-3>, 2010.

637 Iqbal, J., Castellano, M.J., and Parkin, T.B.: Evaluation of photoacoustic infrared spectroscopy

638 for simultaneous measurement of N<sub>2</sub>O and CO<sub>2</sub> gas concentrations and fluxes at the soil

639 surface, *Global Change Biol.*, 19, 327–336, <https://doi.org/10.1111/gcb.12021>, 2013.

640 Jie, D. F., Wei, X., Zhou, H. L., Pan, J. M., and Ying, Y. B.: Research progress on interference

641 in the detection of pollutant gases and improving technology in livestock farms: A review,

642 *Appl. Spectrosc. Rev.*, 52, 101–122, <https://doi.org/10.1080/05704928.2016.1208213>, 2016.

643 Joo H.S., Ndegwa P.M., Neerackal G.M., Wang X., and Harrison J.H.: Effects of manure

644 managements on ammonia, hydrogen sulfide and greenhouse gases emissions from the

645 naturally ventilated dairy barn, *ASABE*, 2, 1302-1311,

646 <https://doi.org/10.13031/aim.20131593447>, 2013.

647 Lambert J.D.: *Vibrational and Rotational Relaxation in Gases*, Clarendon Press, Oxford, 1977.

648 Lin, X., Zhang, R., Jiang, S., El-Mashad, H., and Xin, H.: Emissions of ammonia, carbon

649 dioxide and particulate matter from cage-free layer houses in California, *Atmos. Environ.*,

650 152, 246–255, <https://doi.org/10.1016/j.atmosenv.2016.12.018>, 2017.

651 Li, R., Nielsen, P. V., and Zhang, G. Q.: Effects of airflow and liquid temperature on ammonia

652 mass transfer above an emission surface: experimental study on emission rate, *Bioresource*

653 *Technol.*, 100, 4654–4661, <https://doi.org/10.1016/j.biortech.2009.05.003>, 2009.

654 Liu D., Lokke M.M., Leegaard Riis A., Mortensen K., and Feilberg A.: Evaluation of clay

655 aggregate biotrickling filters for treatment of gaseous emissions from intensive pig

656 production, *J. Environ. Manage.*, 136, 1–8, <https://doi.org/10.1016/j.jenvman.2014.01.023>,  
657 2014.

658 Liu, D., Nyord, T., Rong, L., and Feilberg, A.: Real-time quantification of emissions of volatile  
659 organic compounds from land spreading of pig slurry measured by PTR-MS and wind  
660 tunnels, *Sci. Total. Environ.*, 639, 1079–1087,  
661 <https://doi.org/10.1016/j.scitotenv.2018.05.149>, 2018.

662 Lumasense.: Photoacoustic Gas Monitor - INNOVA 1412i.  
663 [http://www.lumasenseinc.com/FR/produits/gas-sensing/gas-monitoring-](http://www.lumasenseinc.com/FR/produits/gas-sensing/gas-monitoring-instruments/photoacoustic-spectroscopy-pas/photoacoustic-gas-monitor-innova-1412i/)  
664 [instruments/photoacoustic-spectroscopy-pas/photoacoustic-gas-monitor-innova-1412i/](http://www.lumasenseinc.com/FR/produits/gas-sensing/gas-monitoring-instruments/photoacoustic-spectroscopy-pas/photoacoustic-gas-monitor-innova-1412i/).  
665 Accessed 18<sup>th</sup> November, 2018.

666 Malkina, I.L., Kumar, A., Green, P.G., and Mitloehner, F.M.: Identification and quantitation of  
667 volatile organic compounds emitted from dairy silages and other feedstuffs, *J. Environ. Qual.*,  
668 40, 28, <https://doi.org/10.2134/jeq2010.0302>, 2011.

669 Melse, R. W., and Werf, A. W. V. D.: Biofiltration for mitigation of methane emission from  
670 animal husbandry, *Environ. Sci. Technol.*, 39, 5460, <https://doi.org/10.1021/es048048q>,  
671 2005.

672 Moset, V., Cambra-López, M., Estellés, F., Torres, A. G., and Cerisuelo, A.: Evolution of  
673 chemical composition and gas emissions from aged pig slurry during outdoor storage with  
674 and without prior solid separation, *Biosyst. Eng.*, 111, 2–10,  
675 <https://doi.org/10.1016/j.biosystemseng.2011.10.001>, 2012.

676 Ngwabie, N. M., Jeppsson, K. H., Gustafsson, G., and Nimmermark, S.: Effects of animal  
677 activity and air temperature on methane and ammonia emissions from a naturally ventilated

678 building for dairy cows, *Atmos. Environ.*, 45, 6760–6768,  
679 <https://doi.org/10.1016/j.atmosenv.2011.08.027>, 2011.

680 Ngwabie, N.M., Schade, G.W., Custer, T.G., Linke, S., and Hinz, T.: Abundances and flux  
681 estimates of volatile organic compounds from a dairy cowshed in Germany, *J. Environ. Qual.*,  
682 37, 565–573, <https://doi.org/10.2134/jeq2006.0417>, 2008.

683 Ni, J. Q., and Heber, A. J.: Sampling and Measurement of Ammonia at Animal Facilities, *Adv.*  
684 *Agron.*, 98, 201–269, [https://doi.org/10.1016/s0065-2113\(08\)00204-6](https://doi.org/10.1016/s0065-2113(08)00204-6), 2008.

685 Ni, J. Q., Diehl, C. A., Chai, L., Chen, Y., Heber, A. J., Lim, T. T., and Bogan, B. W.: Factors  
686 and characteristics of ammonia, hydrogen sulfide, carbon dioxide, and particulate matter  
687 emissions from two manure-belt layer hen houses, *Atmos. Environ.*, 156,  
688 <https://doi.org/10.1016/j.atmosenv.2017.02.033>, 2017.

689 Norman, M., Hansel, A., and Wisthaler, A.: O<sub>2</sub><sup>+</sup> as reagent ion in the PTR-MS instrument:  
690 Detection of gas-phase ammonia, *Int. J. Mass Spectrom.*, 265, 382–387,  
691 <https://doi.org/10.1016/j.ijms.2007.06.010>, 2007.

692 Osada, T., and Fukumoto, Y.: Development of a new dynamic chamber system for measuring  
693 harmful gas emissions from composting livestock waste, *Water Sci. Technol.*, 44, 79–86,  
694 <https://doi.org/10.2166/wst.2001.0513>, 2001.

695 Osada, T., Rom H.B., and Dahl P.: Continuous measurement of nitrous oxide and methane  
696 emission in pig units by infrared photoacoustic detection, *T. ASAE*, 41, 1109–1114,  
697 <https://doi.org/10.13031/2013.17256>, 1998.

698 Paulot, F., Jacob, D. J., Pinder, R. W., Bash, J. O., Travis, K., and Henze, D. K.: Ammonia  
699 emissions in the United States, European Union, and China derived by high - resolution

700 inversion of ammonium wet deposition data: Interpretation with a new agricultural emissions  
701 inventory (MASAGE\_NH3), J. Geophys. Res., 119, 4343–4364,  
702 <https://doi.org/10.1002/2013JD021130>, 2015.

703 Pearson, J., and Stewart, G. R.: The deposition of atmospheric ammonia and its effects on plants,  
704 New Phytol., 125, 283–305, <https://doi.org/10.1111/j.1469-8137.1993.tb03882.x>, 1993.

705 Picarro.: Technology: Cavity Ring-Down Spectroscopy (CRDS), Link:  
706 [https://www.picarro.com/technology/cavity\\_ring\\_down\\_spectroscopy](https://www.picarro.com/technology/cavity_ring_down_spectroscopy). Accessed 12<sup>th</sup> May,  
707 2018.

708 Phillips, V. R., Lee, D. S., Scholtens, R., Garland, J. A., and Sneath, R. W.: SE—Structures and  
709 Environment : A Review of Methods for measuring Emission Rates of Ammonia from  
710 Livestock Buildings and Slurry or Manure Stores, Part 2: monitoring Flux Rates,  
711 Concentrations and Airflow Rates, J. Agr. Eng. Res., 78, 1–14,  
712 <https://doi.org/10.1006/jaer.2000.0618>, 2001.

713 Pinder, R. W., Adams, P. J., and Pandis, S. N.: Ammonia emission controls as a cost-effective  
714 strategy for reducing atmospheric particulate matter in the Eastern United States, Environ.  
715 Sci. Technol., 41, 380–6, <https://doi.org/10.1021/es060379a>, 2007.

716 Rabaud, N.E., Ebeler, S.E., Ashbaugh, L.L., and Flocchini, R.G.: Characterization and  
717 quantification of odorous and non-odorous volatile organic compounds near a commercial  
718 dairy in California, Atmos. Environ., 37, 933–940, [https://doi.org/10.1016/S1352-2310\(02\)00970-6](https://doi.org/10.1016/S1352-2310(02)00970-6), 2003.

720 Rong L., Liu D., Pedersen E.F., and Zhang G.: Effect of climate parameters on air exchange  
721 rate and ammonia and methane emissions from a hybrid ventilated dairy cow building, Energ.



722 Buildings, 82, 632–643, <https://doi.org/10.1016/j.enbuild.2014.07.089>, 2014.

723 Schilt, S., Thévenaz, L., Niklès, M., Emmenegger, L., and Hüglin, C.: Ammonia monitoring at  
724 trace level using photoacoustic spectroscopy in industrial and environmental applications,  
725 Spectrochim. Acta. A, 60, 3259–3268, <https://doi.org/10.1016/j.saa.2003.11.032>, 2004.

726 Scholtens, R., Jones, C. J. D. M., Lee, D. S., and Phillips, V. R.: Measuring ammonia emission  
727 rates from livestock buildings and manure stores—part 1: development and validation of  
728 external tracer ratio, internal tracer ratio and passive flux sampling methods, Atmos. Environ.,  
729 38, 3003–3015, <https://doi.org/10.1016/j.atmosenv.2004.02.030>, 2004.

730 Seinfeld, J.H.; and Pandis, S.N.: Atmospheric Chemistry and Physics: From Air Pollution to  
731 Climate Change, Wiley-VCH: New York. 1326 pp., ISBN 0-471-17815-2, 1997.

732 Shaw, S.L., Mitloehner, F.M., Jackson, W., Depeters, E.J., Fadel, J.G., Robinson, P.H.,  
733 Holzinger, R., and Goldstein, A.H.: Volatile organic compound emissions from dairy cows  
734 and their waste as measured by proton-transfer-reaction mass spectrometry, Environ. Sci.  
735 Technol., 41, 1310–1316, <https://doi.org/10.1021/es061475e>, 2007.

736 Smith, P., Martino, D., Cai, Z., Gwary, D., Janzen, H., Kumar, P., Mccarl, B., Ogle, S., O'Mara,  
737 F., and Rice, C.: Greenhouse gas mitigation in agriculture, Philos. T. R. Soc. B, 363, 789–  
738 813, <https://doi.org/10.1098/rstb.2007.2184>, 2008.

739 Thomas, C. D., Cameron, A., Green, R. E., Bakkenes, M., Beaumont, L. J., Collingham, Y. C.,  
740 Erasmus, B. F., De Siqueira, M. F., Grainger, A., and Hannah, L.: Extinction risk from climate  
741 change, Nat., 427, 145–148, <https://doi.org/10.1038/nature02121>, 2004.

742 Van Breemen, N., Mulder, J., and Driscoll, C. T.: Acidification and alkalization of soils, Plant  
743 Soil, 75, 283–308, <https://doi.org/10.1007/BF02369968>, 1983.

744 Von Bobruzki, K., Braban, C.F., Famulari, D., Jones, S.K., Blackall, T., Smith, T.E.L., Blom,  
745 M., Coe, H., Gallagher, M., Ghalaieny, M., McGillen, M.R., Percival, C.J., Whitehead, J.D.,  
746 Ellis, R., Murphy, J., Mohacsi, A., Pogany, A., Junninen, H., Rantanen, S., Sutton, M.A., and  
747 Nemitz, E.: Field inter-comparison of eleven atmospheric ammonia measurement techniques,  
748 *Atmos. Meas. Tech.*, 3, 91–112, <https://doi.org/10.5194/amt-3-91-2010>, 2010.

749 Vries, J. W. D., and Melse, R. W.: Comparing environmental impact of air scrubbers for  
750 ammonia abatement at pig houses: A life cycle assessment, *Biosyst. Eng.*, 161, 53–61,  
751 <https://doi.org/10.1016/j.biosystemseng.2017.06.010>, 2017.

752 Wang-Li L., Li Q.-F., Chai L., Cortus E.L., Wang K., Kilic I., Bogan B.W., Ni J.-Q., and Heber  
753 A.J.: The national air emissions monitoring study's Southeast Layer Site: Part III. Ammonia  
754 concentrations and emissions, *T. ASABE*, 56, 1185–1197, [https://](https://doi.org/10.13031/trans.56.9673)  
755 [doi.org/10.13031/trans.56.9673](https://doi.org/10.13031/trans.56.9673), 2013.

756 Yuan, B., Koss, A.R., Warneke, C., Coggon, M., Sekimoto, K., and de Gouw, J.A.: Proton-  
757 Transfer-Reaction Mass Spectrometry: Applications in Atmospheric Sciences, *Chem. Rev.*,  
758 117, 13187–13229, <https://doi.org/10.1021/acs.chemrev.7b00325>, 2017.

759 Zhao, L., Hadlocon, L. J. S., Manuzon, R. B., Darr, M. J., Keener, H. M., Heber, A. J., and Ni,  
760 J.: Ammonia concentrations and emission rates at a commercial poultry manure composting  
761 facility, *Biosyst. Eng.*, 150, 69–78, <https://doi.org/10.1016/j.biosystemseng.2016.07.006>,  
762 2016.

763 Zhao, Y., Pan, Y., Rutherford, J., and Mitloehner, F. M.: Estimation of the Interference in Multi-  
764 Gas Measurements Using Infrared Photoacoustic Analyzers, *Atmos.*, 3, 246–265,  
765 <https://doi.org/10.3390/atmos3020246>, 2012.